Supplement of SOIL, 5, 383–398, 2019
https://doi.org/10.5194/soil-5-383-2019-supplement

SOIL Open Access EGU

Supplement of

Identifying and quantifying geogenic organic carbon in soils – the case of graphite

Jeroen H. T. Zethof et al.

Correspondence to: Jeroen H. T. Zethof (jeroen.zethof@tu-dresden.de)

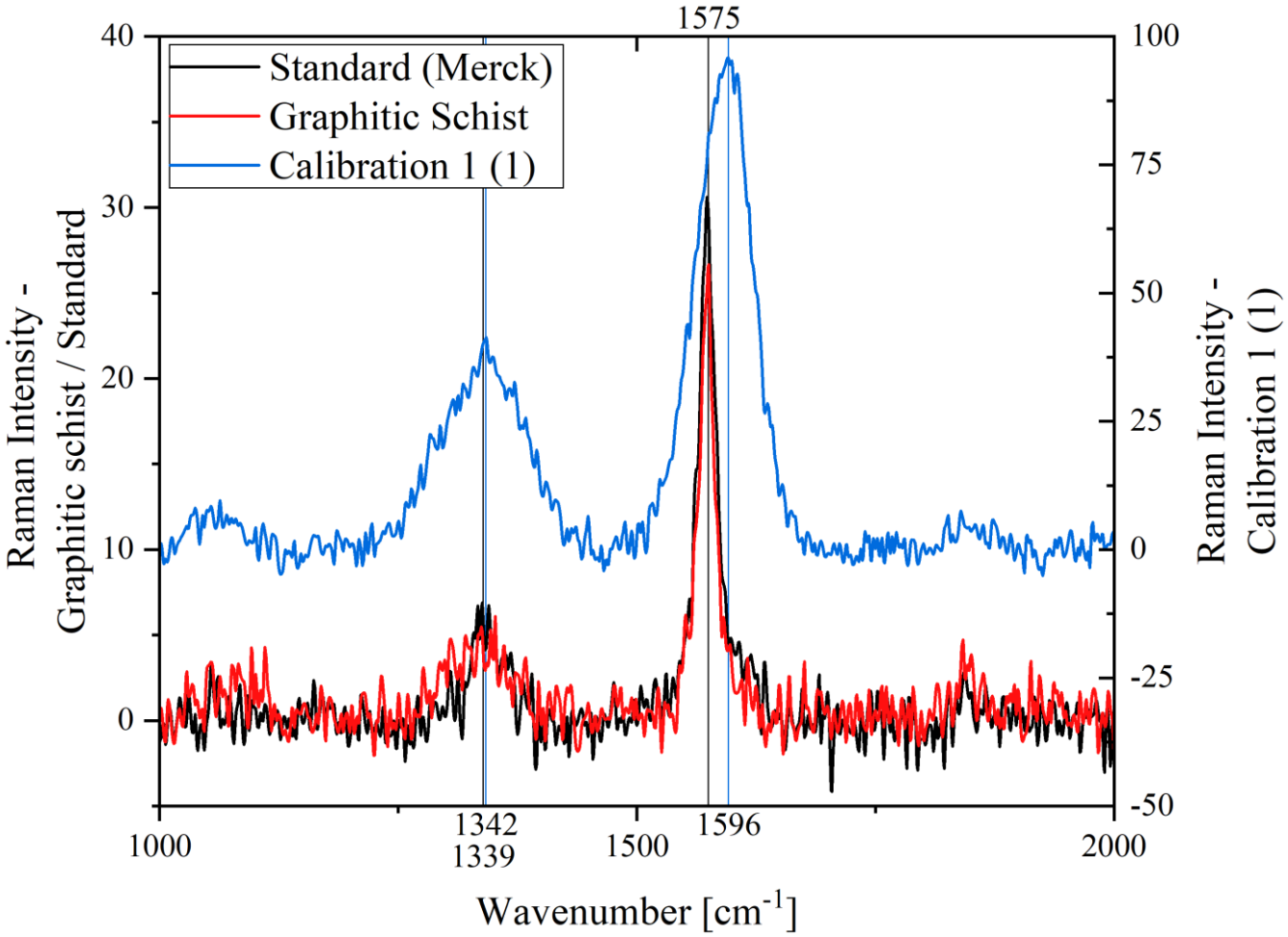

Figure S1. Raman spectra of the graphite standard (black), graphitic schist (red) and soil of calibration set 1 (i.e. natural graphite containing soil, blue). Vertical lines indicate the peaks for amorphous carbon (1342/1339 cm^{-1}) and peaks for graphitic carbon (1575 cm^{-1} standard/schist and 1596 cm^{-1} for soil of calibration set 1). Indicated are the D1 band (1350 cm^{-1}), caused by plane defects and heteroatoms in the carbon structure, G (1580 cm^{-1}), crystalline carbon i.e. pure graphite, and D' band (1620 cm^{-1}), caused by disordered graphitic lattices.

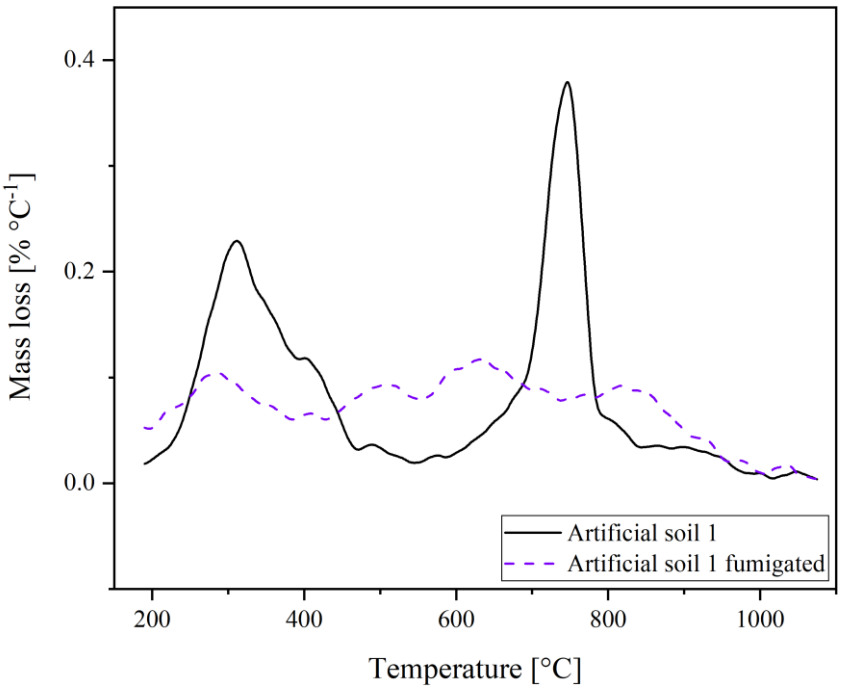

Fig. S2: Thermogravimetric analysis of artificial soil 1 before and after acid fumigation with HCl, as described in section 2.3.

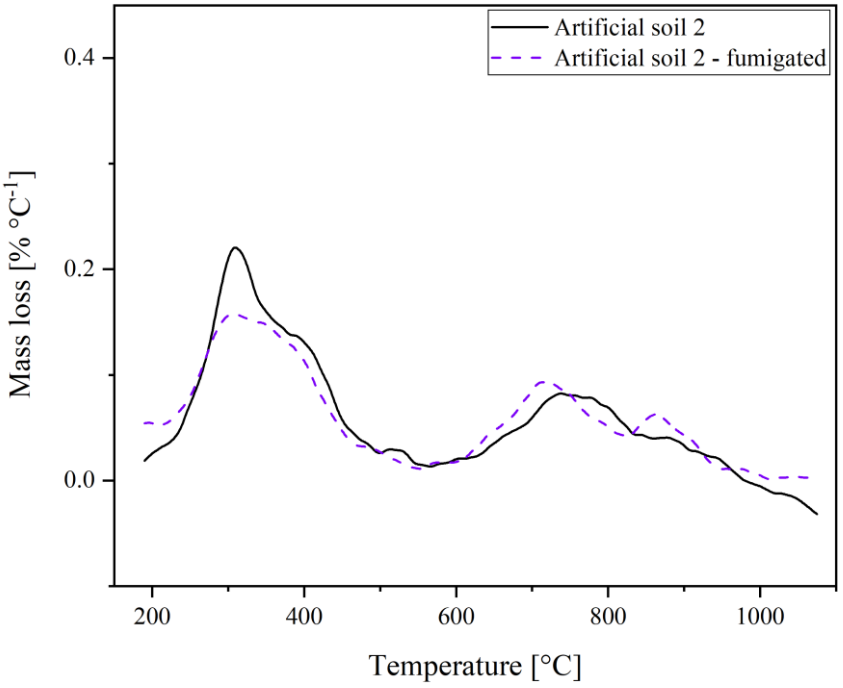

Fig. S3: Thermogravimetric analysis of artificial soil 2, without carbonates, before and after acid fumigation with HCl, as described in section 2.3.

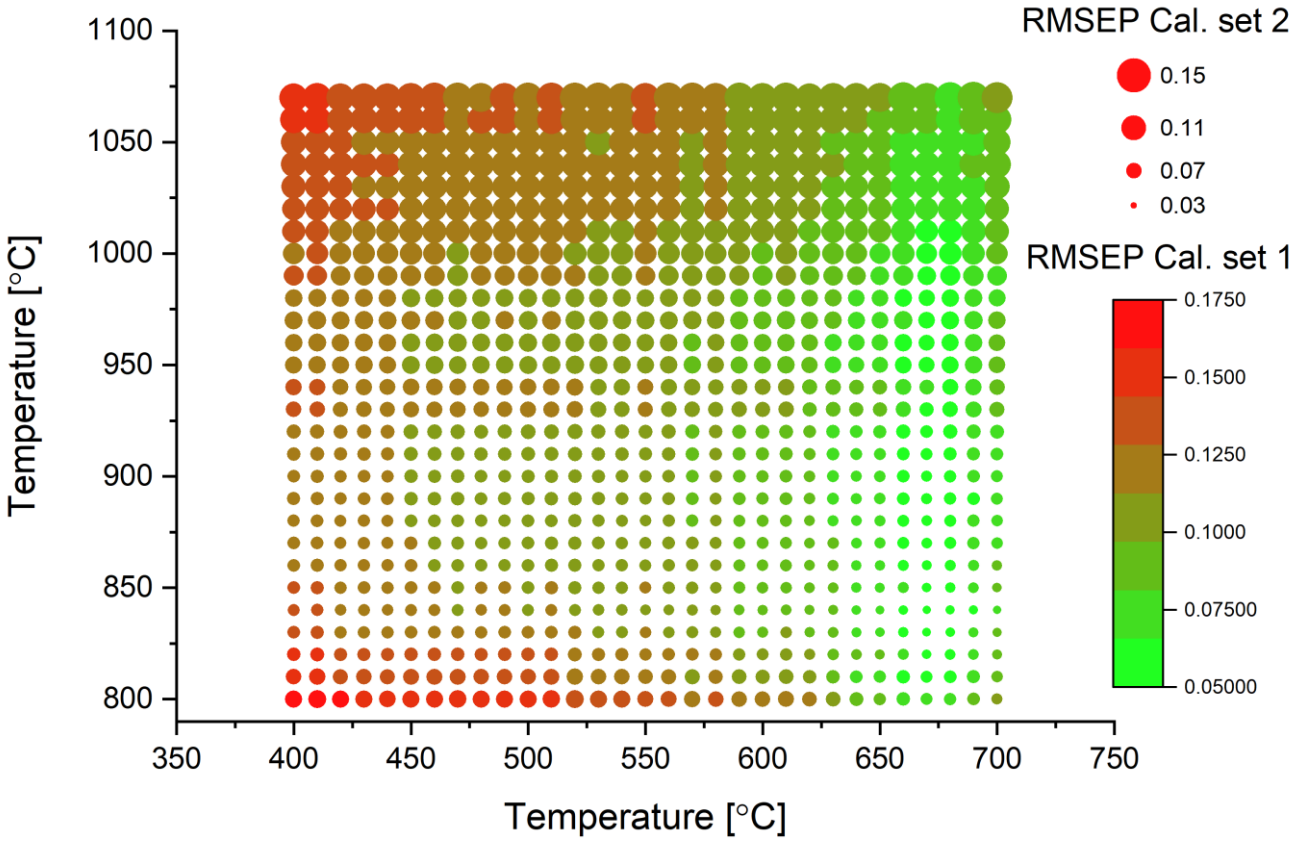

Fig. S4: Exploration of the best TGA temperature range (x – y axis) for creating a graphite content prediction model, based on the root-mean-square error (RMSE) data for calibration set 1 (color) and calibration set 2 (size). The smaller the RMSE, the better the model fitted to the data.

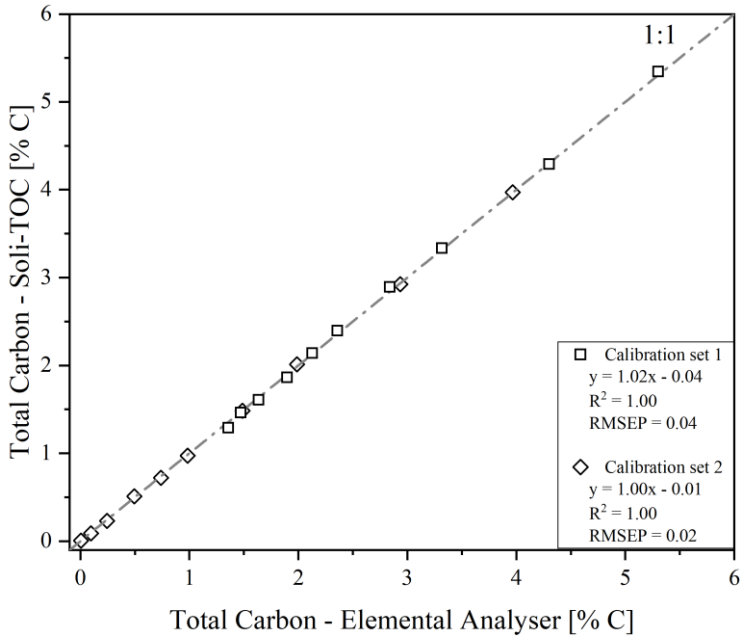

Fig. S5: Total carbon of the two calibrations sets as measured by the Elemental analyser and Soli-TOC device.